Phosphorylation of H2A by Bub1 Prevents Chromosomal Instability Through Localizing Shugoshin

Shigehiro A. Kawashima,[1] Yuya Yamagishi,[1,2]* Takashi Honda,[1,3]* Kei-ichiro Ishiguro,[1] Yoshinori Watanabe[1,2,3]†

Bub1 is a multi-task protein kinase required for proper chromosome segregation in eukaryotes. Impairment of Bub1 in humans may lead to chromosomal instability (CIN) or tumorigenesis. Yet, the primary cellular substrate of Bub1 has remained elusive. Here, we show that Bub1 phosphorylates the conserved serine 121 of histone H2A in fission yeast *Schizosaccharomyces pombe*. The *h2a-SA* mutant, in which all cellular H2A-S121 is replaced by alanine, phenocopies the *bub1* kinase-dead mutant (*bub1-KD*) in losing the centromeric localization of shugoshin proteins. Artificial tethering of shugoshin to centromeres largely restores the *h2a-SA* or *bub1-KD*–related CIN defects, a function that is evolutionally conserved. Thus, Bub1 kinase creates a mark for shugoshin localization and the correct partitioning of chromosomes.

The precise partition of chromosomes to daughter cells is essential for maintaining the integrity of genomes (*1*, *2*). When sister chromatid kinetochores are captured by spindle microtubules from opposite poles (bipolar attachment), sister chromatids are held together by the cohesin complex (*3*–*5*). The shugoshin protein phosphatase 2A (PP2A) complex protects centromeric cohesin during mitotic prophase in animal cells and more generally during meiosis I (*6*–*8*). When all sister chromatids have achieved biorientation, the anaphase-promoting complex (APC)–dependent degradation of securin liberates separase, which cleaves the cohesin subunit Rad21 (or Rec8 in meiosis), resulting in the separation of sister chromatids (*3*, *4*, *9*). The spindle assembly checkpoint (SAC) senses unattached kinetochores or a lack of tension and, by inhibiting the APC, prevents premature entry to anaphase. Aurora B destabilizes erroneous attachments and activates the SAC, which monitors the lack of tension (*10*, *11*). Shugoshin also loads the Aurora B complex to centromeres and ensures the bipolar attachment of kinetochores (*12*–*14*).

The conserved SAC protein kinase Bub1 is a tumor suppressor (*15*, *16*). The N-terminal non-kinase domain of Bub1 recruits SAC components to kinetochore, whereas Bub1 kinase activity plays a role in chromosome congression and an auxiliary role in SAC activation (*17*–*22*). The centromeric localization of shugoshin seems to depend on Bub1 (*14*, *23*–*26*). Although several candidates for Bub1 substrates have been suggested (*14*, *22*, *27*), the canonical substrate still remains to be identified even in genetically tractable organisms such as yeast. Therefore, the molecular entity of the downstream of Bub1 remains a longstanding enigma and controversial issue.

Bub1 phosphorylates H2A Ser^{121}. To identify substrates of the Bub1 kinase, we prepared a chromatin fraction from a fission yeast cell extract and mixed it with [γ-^{32}P] adenosine 5′-triphosphate (ATP) and recombinant Bub1 protein (*28*). A major phosphorylation was detected in the ~15 kDa range, close to histone H2A and H2B (Fig. 1A). This phosphopeptide was precipitated by an antibody to H2A (Fig. 1B). We confirmed this by tagging endogenous H2A with FLAG (H2Aα and H2Aβ, encoded by *hta1*$^+$ and *hta2*$^+$, were both tagged) and immunoblotting the major phosphopeptide, which was migrated more slowly in the *h2a*$^+$*-flag* strain (Fig. 1C). Recombinant H2A proteins are efficiently phosphorylated by Bub1 but not by Aurora B in vitro (Fig. 1D). Phosphorylation by Bub1 is abolished in H2A lacking the C-terminal tail but not in H2A lacking the N-terminal tail (fig. S1). Amino acid substitution and phospho–amino acid analysis identified Ser 121 as the phosphorylation site of H2A by Bub1 in vitro (Fig. 1, E and F). Antibodies that specifically recognize phosphorylated H2A-S121 (H2A-pS121) gave an H2A-pS121 signal in wild-type cells. This signal was abolished in cell extracts prepared from *h2a-SA* cells, in which Ser 121 is replaced with alanine (H2A-S121A) in both the *hta1*$^+$ and *hta2*$^+$ genes (Fig. 1G). We made a kinase–dead point mutation allele of *bub1* (*bub1-KD*) (fig. S2) and examined the phosphorylation of H2A-S121 in cell extracts prepared from *bub1-KD* cells. H2A-S121 phosphorylation was completely abolished in *bub1-KD* cells, although a similar amount of H2A was detected (Fig. 1G). Thus, H2A-S121 is an in vivo substrate of Bub1 kinase in fission yeast.

***h2a-SA* phenocopies *bub1-KD*.** Although *h2a-SA* cells are viable, they show a similar level of hypersensitivity to the microtubule-destabilizing drug thiabendazole (TBZ) as *bub1-KD* cells but to a lesser extent than *bub1*Δ cells (Fig. 2A). *bub1-KD* cells, but not *bub1*Δ cells, arrested at prometaphase when spindle formation was abolished (Fig. 2B). However, when sister chromatid cohesion was inactivated and thus tension was

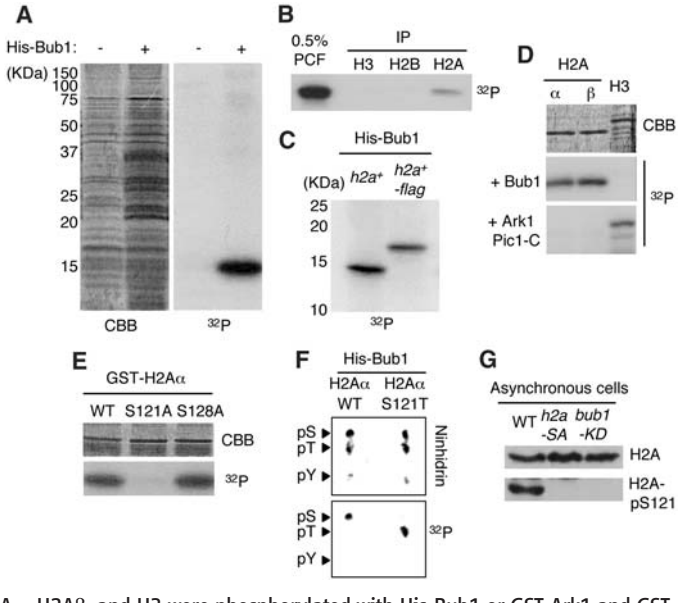

Fig. 1. H2A-S121 is phosphorylated by Bub1. (**A**) Chromatin fractions were incubated with or without recombinant His-Bub1 in the presence of [γ-^{32}P]ATP. The incorporation of the radioactive phosphate group was visualized by means of autoradiography (^{32}P), and protein loading was analyzed through staining with Coomassie Brilliant Blue (CBB). (**B**) The phosphorylated chromatin fraction (PCF) was denatured and immunoprecipitated with the indicated antibodies. (**C**) Chromatin fractions from *h2a*$^+$ or *h2a*$^+$*-flag* cells were phosphorylated as in (A). (**D**) Recombinant H2Aα, H2Aβ, and H3 were phosphorylated with His-Bub1 or GST-Ark1 and GST-Pic1-C. (**E**) The indicated mutants of GST-H2Aα were phosphorylated with His-Bub1. (**F**) Phospho–amino acid analysis of H2Aα and H2Aα-S121T phosphorylated by Bub1. (**G**) Cell extracts prepared from the indicated cells were immunoblotted for H2A-pS121 and H2A.

[1]Laboratory of Chromosome Dynamics, Institute of Molecular and Cellular Biosciences, University of Tokyo, Yayoi, Tokyo 113-0032, Japan. [2]Graduate Program in Biophysics and Biochemistry, Graduate School of Science, University of Tokyo, Yayoi, Tokyo 113-0032, Japan. [3]Graduate School of Agricultural and Life Science, University of Tokyo, Yayoi, Tokyo 113-0032, Japan.

*These authors contributed equally to this work.
†To whom correspondence should be addressed. E-mail: ywatanab@iam.u-tokyo.ac.jp

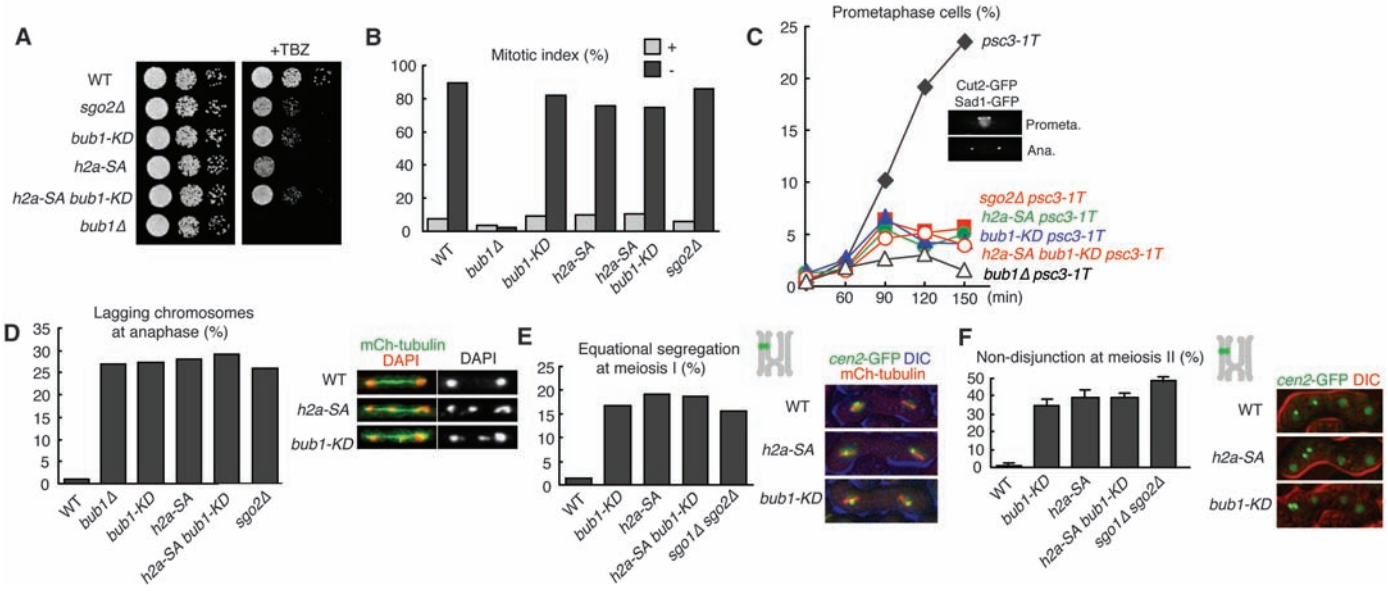

Fig. 2. Similar chromosomal instability (CIN) defects of *bub1-KD*, *h2a-SA*, and shugoshin mutants. (**A**) Serial dilution assay (12.5 μg/ml TBZ). (**B**) The indicated cells carrying a mutation of β-tubulin (*nda3-KM311*) were cultured at permissive temperature (+) or restrictive temperature (–) and scored for mitotic index (n > 200 cells). (**C**) The indicated temperature-sensitive cohesin mutants (*psc3-1T*) were arrested at the G_1/S phase by adding hydroxyurea (HU) and released by increasing the temperature. Prometaphase (spindle pole body–duplicated and securin/Cut2 positive) cells were counted at each time point (n > 200 cells). (**D**) The indicated strains expressing mCherry-Atb2 (α2-tubulin) were examined for frequencies of lagging chromosomes in anaphase cells (n > 100 cells). Examples are shown at the right. (**E**) One of the homologs marked with *cen2*–green fluorescent protein (GFP) was monitored for segregation during meiosis I in the indicated zygotes. The number of cells that had undergone equational segregation in meiosis I was examined by monitoring metaphase II cells (n > 100 zygotes). (**F**) One of the homologs marked with *cen2*-GFP was monitored for segregation during meiosis II in the indicated zygotes (n > 200 zygotes).

Fig. 3. Forced enrichment of shugoshins in centromeres suppresses the CIN defects of *bub1-KD* or *h2a-SA* cells. (**A**) The signals of Sgo2-GFP expressed from the endogenous promoter were measured in metaphase in the indicated cells. Error bars represent SEM (n = 16 cells). (**B**) Sgo1-GFP expressed from the endogenous promoter was detected in metaphase I in the indicated cells. The metaphase I spindle was visualized with mCherry-Atb2. Sgo1 signals were detected only in wild-type cells (n > 50 zygotes). (**C**) The indicated *pcs3-1T* strains were arrested at the G_1/S phase and released by raising the temperature. Prometaphase cells were counted at each time point (n > 200 cells). (**D**) The indicated cells were examined for frequencies of lagging chromosomes at anaphase (n > 100 cells). (**E**) The signal intensity of Ark1-GFP in metaphase cells was measured. Error bars represent SEM (n > 25 cells). (**F**) One of the homologs marked with *cen2*-GFP was monitored for segregation during meiosis II in the indicated zygotes (n > 200 zygotes). (**G**) Par1-mCherry was detected at metaphase I. (**H**) Schematic depiction of the Bub1 pathway regulating chromosome segregation.

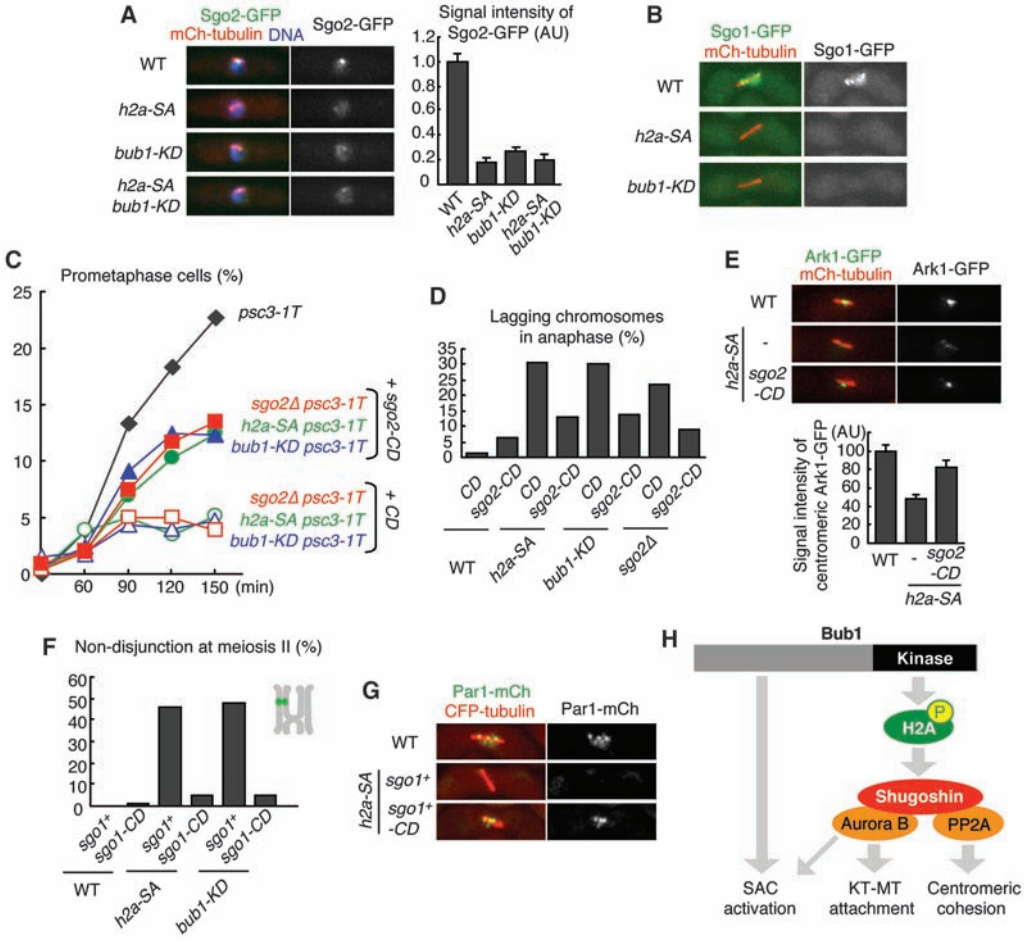

abolished between sister chromatids, *bub1-KD* cells showed the same defect in activating the SAC as *bub1*Δ cells (Fig. 2C). Thus, although the N-terminal non-kinase domain of Bub1 may fully contribute to the SAC, the kinase activity plays a limited role in the SAC activation. In this regard, *h2a-SA* cells behave exactly like *bub1-KD* cells (Fig. 2, B and C). Bub1 is required for the proper attachment of the kinetochore to microtubules (*29*), which was similarly impaired in both *bub1-KD* and *bub1*Δ cells (Fig. 2D), implying that the attachment is predominantly governed by the kinase activity rather than non-kinase function of Bub1. *h2a-SA* cells show similar defects in attachment (Fig. 2D).

In meiosis I, sister kinetochores are captured from the same pole (monopolar attachment), whereas homologous chromosomes are captured from the opposite poles. Bub1 ensures monopolar attachment by preventing merotelic attachment of paired sister kinetochores (*30*). At anaphase I, sister chromatid cohesin (or Rec8 cohesin) is released only along the arms, whereas centromeric cohesin is persistent, which ensures faithful disjunction at meiosis II. Bub1 is required for this protection of Rec8 cohesin at centromeres (*31*). We confirmed that *bub1-KD* cells display defects in the monopolar attachment at meiosis I (Fig. 2E) and in the centromeric protection of Rec8 cohesin (fig. S3), which results in nondisjunction at meiosis II (Fig. 2F). *h2A-SA* cells show nearly identical defects in monopolar attachment and centromeric protection (Fig. 2, E and F), whereas the phospho-mimic *h2a-SE* mutation suppresses the defect of centromeric protection in *bub1-KD* cells (fig. S4). Because the *bub1-KD h2a-SA* double mutant shows no additive defects in either mitotic or meiotic chromosome segregation (Fig. 2), these results argue that H2A-S121 phosphorylation and Bub1 kinase activity act in the same pathway and that H2A is a predominant cellular substrate for Bub1 kinase in fission yeast.

H2A-S121 phosphorylation regulates shugoshin localization. Bub1 is required for the localization of shugoshin (*14*, *23*–*26*, *32*), and H2A-pS121 might mediate this linkage. Fission yeast shugoshin Sgo2 is expressed in both mitosis and meiosis and is required for loading the Aurora B complex to centromeres, preventing merotelic attachment, and activating the SAC that senses lack of tension (*12*, *13*, *30*), whereas Sgo1 is meiosis-specific and required for loading PP2A and protecting centromeric cohesion presumably by dephosphorylating cohesin (*6*, *7*). The centromeric localization of Sgo2 is abolished in *h2a-SA* cells, such as in *bub1-KD* cells, during both mitosis and meiosis (Fig. 3A and fig. S5), and the mitotic defects in the SAC and kinetochore attachment of *h2a-SA* or *bub1-KD* cells are reproduced in *sgo2*Δ cells (Fig. 2, B to D). Similarly, the localization of meiosis-specific Sgo1 is abolished in *bub1-KD* or *h2a-SA* zygotes (Fig. 3B), accounting for the nearly identical defects in centromeric protection during meiosis

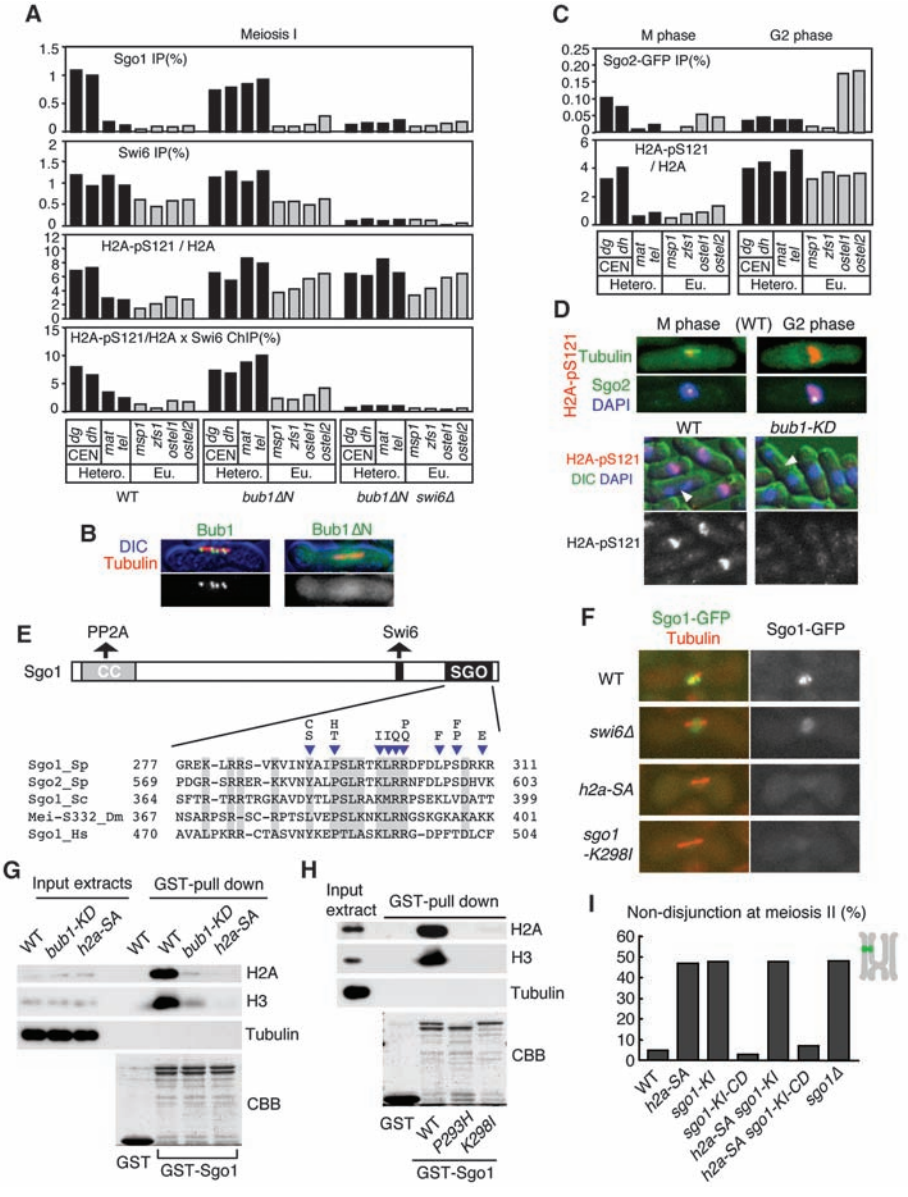

Fig. 4. Association between the SGO motif and nucleosomes containing H2A-pS121 is required for the chromosomal localization of shugoshin. (**A**) ChIP analysis was used to measure Sgo1, Swi6, H2A-pS121, and H2A throughout the heterochromatic centromere (*dg* and *dh*), mating type locus (*mat*), and telomere (*tel*); euchromatic arm region (*msp1* and *zfs1*); and outer subtelomere (*ostel1* and *ostel2*) in the indicated strains at metaphase I. Values of H2A-pS121/H2A multiplied by Swi6 ChIP (in percent) are compared with those of Sgo1 ChIP (in percent), revealing a good correlation along the chromosome. (**B**) Bub1-GFP and Bub1ΔN-GFP were detected in cells at metaphase I. (**C**) ChIP analysis was used to measure Sgo2, Swi6, H2A-pS121, and H2A in asynchronous (G_2) or M phase–arrested (M) *nda3-KM311* cells. (**D**) Immunostaining for Sgo2, H2A-pS121, tubulin, and DNA in wild-type cells (top) and for H2A-pS121 and DNA in the indicated cells (bottom). Arrowheads indicate anaphase cells. (**E**) A schematic of the Sgo1 protein showing the PP2A-interacting coiled-coil region (CC), Swi6/HP1–interacting motif (black box), and SGO motif (SGO). Arrowheads indicate the mutations isolated in a genetic screening (fig. S13), which abolish Sgo1 localization. (**F**) Sgo1 localization was examined at metaphase I in the indicated strains. (**G**) Cell extracts prepared from the indicated strains were pulled down with GST-Sgo1 or GST and analyzed by means of immunoblotting with antibodies to H3, H2A, and tubulin. Input extracts are also shown (0.5%). (**H**) Cell extracts prepared from wild-type cells were pulled down with the indicated Sgo1 mutant proteins fused with GST and analyzed as in (G). (**I**) One of the homologs marked with *cen2*-GFP was monitored for segregation during meiosis II in the indicated zygotes at 26.5°C (n > 200 zygotes).

of these mutants (Fig. 2F and fig. S3). Consistently, the centromeric localization of shugoshin effectors Aurora B and PP2A is impaired in *h2a-SA* and *bub1-KD* cells such as in shugoshin-deleted cells (fig. S6). We conclude that shugoshin localization and functions are largely abolished in *h2a-SA* cells as well as in *bub1-KD* cells.

If localization of shugoshin is the major function of H2A-S121 phosphorylation, then forced localization of Sgo1 and Sgo2 should restore the defects in *h2a-SA* or *bub1-KD* cells. We fused Sgo1 and Sgo2 C-terminal ends to the chromo domain (CD), which binds to Lys-9–methylated histone H3 principally located at the centromeric heterochromatin. Sgo2-CD, which localizes at centromeres in the absence of H2A-S121 phosphorylation (fig. S7), partially (~60%) restored the defects in the SAC and kinetochore attachment in *h2a-SA* and *bub1-KD* cells during mitosis (Fig. 3, C and D). Likewise, the expression of Sgo2-CD partially (~60%) complements *sgo2*Δ (Fig. 3, C and D). Given that Sgo2 is mainly required for the centromeric localization of Aurora B and that this localization is indeed restored by Sgo2-CD in *h2a-SA* cells (Fig. 3E), our results imply that one of the functions of Bub1 kinase in vivo is the localization and/or activation of Aurora B at centromeres, which regulates attachment and the SAC. Moreover, nondisjunction at meiosis II, which originates from defects in centromeric protection during meiosis I, was fully restored in *h2a-SA* or *bub1-KD* cells by expressing Sgo1-CD and restoring PP2A localization at centromeres (Fig. 3, F and G). Collectively, these results argue that the primary readout of Bub1 kinase activity in vivo is the localization of both Sgo1 and Sgo2 to centromeres, in which they recruit PP2A and Aurora B, respectively. H2A-pS121 is the principal mediator of the crucial link between Bub1 kinase and the shugoshin action.

H2A-pS121 nucleosomes associate with shugoshin. The centromeric localization of Sgo1 in meiosis I depends largely on the specific association with heterochromatin protein Swi6 (*Schizosaccharomyces pombe* HP1 homolog) (*33*). However, chromatin immunoprecipitation (ChIP) assay indicates that Swi6 localizes not only to the centromeric region but also to the mating type (*mat*) locus and telomeres (*34*), despite the fact that Sgo1 is exclusively centromeric (*33*) (Fig. 4A). H2A-S121 phosphorylation is most enriched at the centromere but not other heterochromatic regions at metaphase I (Fig. 4A), which is consistent with the fact that Bub1 localizes at centromeres at this stage (*31*) (fig. S8) and that this phosphorylation as well as Sgo1 localization are totally dependent on Bub1 (fig. S8). To delineate the requirement of H2A-S121 phosphorylation and heterochromatin

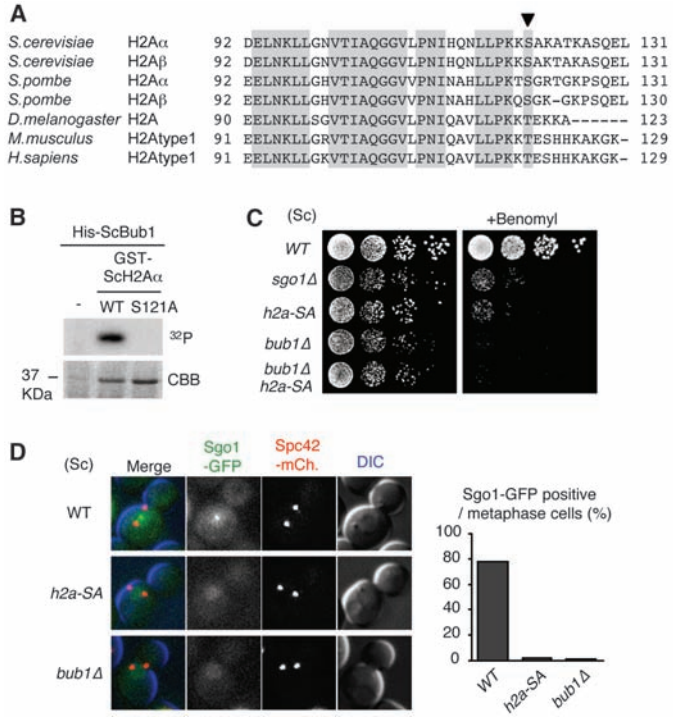

Fig. 5. Bub1-H2A-shugoshin pathway is conserved in budding yeast. (**A**) Alignment of the C-tail of histone H2A (amino acids are numbered excluding the first methionine). Ser 121 (arrowhead) and the preceding sequence are widely conserved among eukaryotes. (**B**) GST-ScH2A (wild-type or S121A) proteins were incubated with His-ScBub1 in the presence of [γ-^{32}P]ATP for 30 min at 30°C. (**C**) Serial dilution assay (10 μg/ml Benomyl). (**D**) ScSgo1-GFP was detected at metaphase (mitotic spindle indicated by separated Spc42 signals) in wild-type, *h2a-SA*, and *bub1* cells. Quantification of Sgo1-GFP–positive cells at metaphase is shown (n > 100 cells).

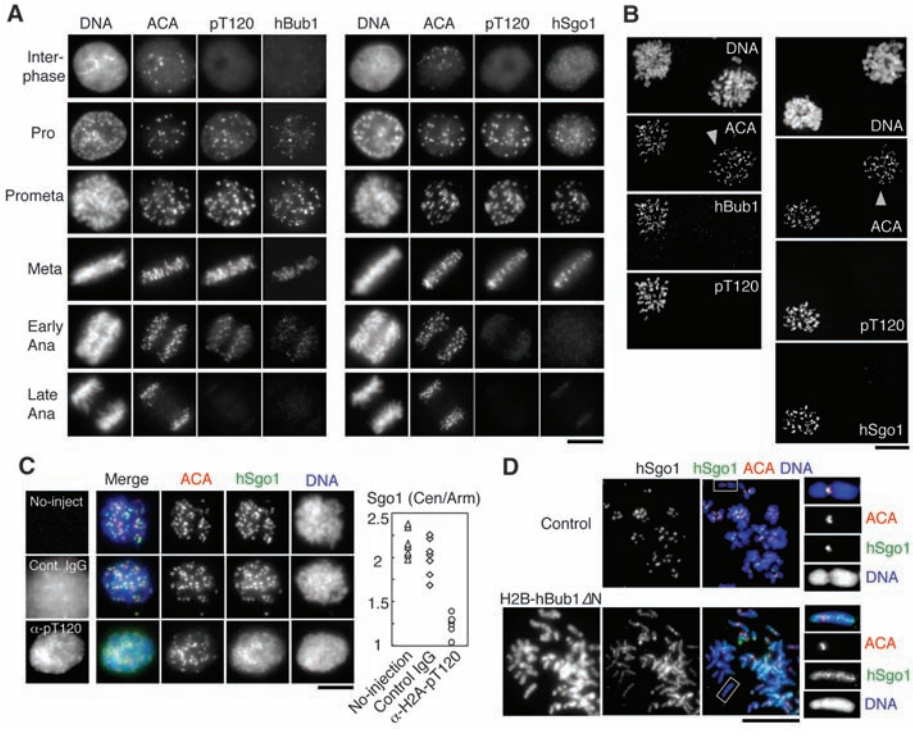

Fig. 6. Bub1-H2A-shugoshin pathway is conserved in humans. (**A**) Cycling HeLa cells were spun onto glass slides after fixation and stained with antibody to H2A-pT120 and anti-centromere antibodies (ACA) as well as antibodies to hBub1 (left) or hSgo1 (right). DNA was counterstained with Hoechst 33342. (**B**) HeLa cells treated with Bub1 siRNA were arrested at prometaphase by nocodazole and MG132 for 3 hours. Immunostaining was performed as in (A). Arrowheads indicate a Bub1-negative cell (left) and an H2A-pT120 negative cell (right), respectively. (**C**) Cells injected with antibody to H2A-pT120 or control immunoglobulin G (IgG) were arrested at prometaphase by nocodazole and stained with antibody to hSgo1 and ACA. The injected antibodies and DNA were also stained. The ratio of centromere and arm Sgo1 signals was quantified. (**D**) HeLa cells expressing H2B-Bub1ΔN-GFP were depleted for endogenous Bub1 by means of RNA interference, subjected to chromosome spreads, and stained with antibody to hSgo1 and ACA. Magnified images of paired sister chromatids are shown on the left. Scale bars, 10 μm.

for Sgo1 localization, we expressed a Bub1-kinase domain lacking the N-terminal regulatory region (Bub1ΔN), which showed uniform localization within the nucleus at metaphase I (Fig. 4B). ChIP assay indicated that the phosphorylation of H2A-S121 is elevated along the entire chromosome length in *bub1ΔN* cells at metaphase I (Fig. 4A). Consequently, Sgo1 localization, which is usually limited to the centromeres, extended to all heterochromatic regions including the *mat* locus and telomeres but not to euchromatic regions (Fig. 4A). The expanded Sgo1 localization was overall abolished by introducing the *swi6*Δ mutation (Fig. 4A). These results indicate that the localization of Sgo1 can largely be defined by a synergetic action of Swi6 and H2A-pS121 (Fig. 4A). The pattern of H2A-pS121 is invariable in *swi6*Δ cells (Fig. 4A and fig. S8), and heterochromatin formation is intact in *h2a-SA* cells (fig. S9), implying that these two pathways are assembled independently and converge into the regulation of the Sgo1 localization.

The regulation of Sgo2 localization is not identical to that of Sgo1 because Sgo2 locates at the outer subtelomeric region in the G_2 phase in a heterochromatin-independent manner (Fig. 4C and fig. S10) while accumulating at centromeres in the M phase, depending on Bir1 (a subunit of the chromosome passenger complex) (*12*, *13*). Crucially, however, the localization of Sgo2 in both G_2 and M phases is largely abolished in *bub1-KD* and *h2a-SA* cells (Fig. 3A and fig. S11). These results indicate that H2A-pS121 promotes the association of Sgo2 with chromatin, regardless of whether it is centromeric or outer subtelomeric. H2A-S121 is phosphorylated along the entire chromosome length in the G_2 phase, whereas it is limited to centromeres in the M phase (Fig. 4, C and D), and both phosphorylations are dependent on Bub1 (Fig. 4D and fig. S12). Thus, phosphorylation of H2A-S121 directs the chromosomal association of shugoshin, whereas additional factors such as heterochromatin, Bir1, or some outer subtelomeric chromatin may affect localization and timing. Enrichment of H2A-pS121 at centromeres during the M phase, which is carried out by the accumulation of Bub1, is crucial in order to restrain the shugoshin localization to centromeres at this stage.

Shugoshin family proteins, albeit conserved among all eukaryotes, share limited similarities in amino acid sequence in the basic region near the C terminus, which we now denote the SGO (shugoshin) motif (Fig. 4E). Screening for mutations that abolish Sgo1 localization (fig. S13), we identified several intragenic mutations, all of which mapped in the SGO motif (Fig. 4E). The mutant proteins preserved the ability to associate with Swi6 in the immunoprecipitation assay (fig. S14), which is consistent with the fact that the Swi6-interacting sequences locate outside the SGO motif of Sgo1 (*33*) (Fig. 4E). Analogous mutations within the SGO motif of Sgo2 abolished the chromatin localization (fig. S11). Although we could not detect the association of nucleosomes with Sgo1 in the immunoprecipitation assay, we could detect it in a pull-down assay, suggesting that their association is not stable. The glutathione *S*-transferase (GST)–Sgo1 protein pulls down the nucleosomes from cell extracts prepared from wild-type cells but not from cell extracts prepared from *bub1-KD* or *h2a-SA* cells (Fig. 4G). Moreover, the mutations in the SGO motif (Sgo1-P293H and -K298I) lost the ability to pull down the nucleosomes even from wild-type cell extracts (Fig. 4H). These results indicate that Sgo1 associates with nucleosomes containing H2A-pS121 through the conserved SGO motif, although further molecular details of the association remain to be studied. To delineate the requirement of the SGO motif for protein function, we fused Sgo1-K298I with the CD and expressed it from the endogenous promoter. Sgo1-K298I-CD can perform its full function in protecting cohesion, and this is also true in *h2a-SA* cells (Fig. 4I). These results argue that the conserved SGO motif is required exclusively for shugoshin localization.

Conservation of the Bub1-H2A-shugoshin pathway. The requirement of Bub1 for shugoshin localization is conserved in budding yeast *Saccharomyces cerevisiae* (*26*, *32*), which lacks the HP1 protein. Recombinant ScH2A was phosphorylated by Bub1 in vitro at the conserved Ser 121 (Fig. 5, A and B). To examine the conservation of the Bub1-H2A-shugoshin pathway, we constructed budding yeast *h2a-SA* strain by expressing mutant H2A-S121A from the low copy centromere-plasmid in cells, in which all H2A genes were deleted (*35*). Like budding yeast *Scsgo1*Δ cells (*36*), *Sch2a-SA* cells were viable and showed sensitivity to the spindle-poison benomyl, though to a lesser extent than *Scbub1*Δ cells (Fig. 5C). These results mirror those in fission yeast. Crucially, ScSgo1 localization was abolished in *Sch2a-SA* cells as well as in *Scbub1*Δ cells (Fig. 5D). Together, these results suggest that shugoshin localization and function are also mediated by Bub1 and H2A phosphorylation in budding yeast.

We next investigated the conservation of the Bub1 kinase pathway in mammals. Because human H2A is phosphorylated by hBub1 in vitro at the conserved Thr 120 (equivalent to yeast H2A-S121), we raised antibodies that recognize this phosphorylation (fig. S15). Immunostaining of HeLa cells indicated that H2A-pT120 colocalizes with hBub1, which together with hSgo1 accumulate at centromeres during prometa- and metaphase in the cell cycle (Fig. 6A). The staining of H2A-pT120 as well as hSgo1 is abolished selectively in hBub1-depleted cells, but not in hBub1-positive cells, after treatment with hBub1 small interfering RNA (siRNA) (Fig. 6B). The injection of antibody to H2A-pT120 interferes with the centromeric localization of hSgo1 (Fig. 6C), suggesting that H2A-pT120 plays a role in hSgo1 localization at centromeres. Moreover, when the Bub1 kinase domain (hBub1ΔN) was fused with H2B and ectopically localized on the chromosome arms in Bub1-depleted cells, H2A-T120 was extensively phosphorylated on the whole chromosome (fig. S16), indicating that the localization of hBub1 kinase usually defines the centromere-specific phosphorylation of H2A-T120. Accordingly, hSgo1 localized along the whole chromosome length in H2B-hBub1ΔN cells (Fig. 6D), indicating that H2A-pT120 plays a predominant role in defining shugoshin localization sites on the human chromosomes, although HP1 may contribute to the maintenance of shugoshin at centromeres (*33*). To examine the conservation in meiosis, we stained mouse spermatocytes to localize mBub1, H2A-pT120, and mSgo2 [a predominant shugoshin in meiotic cells (*37*, *38*)]. H2A-pT120 and mSgo2 accumulate at centromeres during prometa- and metaphase I, when mBub1 accumulates at centromeres (fig. S17). Collectively, these results suggest that H2A-pT120 is an in vivo substrate of Bub1 kinase in mammals and that shugoshin localization at centromeres depends on the Bub1-dependent phosphorylation of H2A-T120 in somatic cells and presumably in germ cells as well.

Discussion. We report here that the conserved C-tail of histone H2A is a primary cellular substrate of Bub1 kinase because almost all *bub1-KD* defects including the SAC, kinetochore attachment, and centromeric protection are precisely phenocopied in *h2a-SA* cells of fission yeast. Because most mitotic and meiotic defects associated with *bub1-KD* or *h2a-SA* are efficiently suppressed by tethering shugoshin proteins at centromeres, we reason that the centromeric localization of shugoshin is the ultimate readout of the kinase activity of Bub1 in fission yeast. Analyses of budding yeast and mammalian cells suggest that this cascade is evolutionally conserved. A previous study in *Drosophila* identified nucleosomal histone kinase-1 (NHK-1) as the kinase for H2A-T119 (equivalent to fission yeast H2A-S121) in vitro (*39*), although this kinase is not relevant to the phosphorylation of H2A-T119 in mitotic cells (*40*). Our study suggests that the mitotic kinase for H2A in *Drosophila* may be Bub1. Previous mutational analyses of budding yeast histone H2A suggest that H2A-S121 plays a role in DNA repair (*41*). Consistently, we found that *bub1-KD* and *h2a-SA* cells, but not *sgo2*Δ cells, show sensitivity to a DNA-damaging agent (fig. S18), implying that the phosphorylation of H2A-S121 by Bub1 plays an additional role in DNA repair during interphase. Our findings in fission yeast mitosis and meiosis spotlight a crucial link between H2A phosphorylation and chromosomal instability, which may lead to tumorigenesis or birth defects in humans, and therefore are useful for future studies in those fields.

References and Notes

1. K. W. Yuen, B. Montpetit, P. Hieter, *Curr. Opin. Cell Biol.* **17**, 576 (2005).
2. A. J. Holland, D. W. Cleveland, *Nat. Rev. Mol. Cell Biol.* **10**, 478 (2009).
3. K. Nasmyth, C. H. Haering, *Annu. Rev. Biochem.* **74**, 595 (2005).

4. J. M. Peters, A. Tedeschi, J. Schmitz, *Genes Dev.* **22**, 3089 (2008).
5. I. Onn, J. M. Heidinger-Pauli, V. Guacci, E. Unal, D. E. Koshland, *Annu. Rev. Cell Dev. Biol.* **24**, 105 (2008).
6. T. S. Kitajima *et al*., *Nature* **441**, 46 (2006).
7. C. G. Riedel *et al*., *Nature* **441**, 53 (2006).
8. Y. Watanabe, *Curr. Opin. Cell Biol.* **17**, 590 (2005).
9. F. Uhlmann, *Curr. Biol.* **13**, R104 (2003).
10. T. U. Tanaka, *Chromosoma* **117**, 521 (2008).
11. B. A. Pinsky, C. Kung, K. M. Shokat, S. Biggins, *Nat. Cell Biol.* **8**, 78 (2006).
12. V. Vanoosthuyse, S. Prykhozhij, K. G. Hardwick, *Mol. Biol. Cell* **18**, 1657 (2007).
13. S. A. Kawashima *et al*., *Genes Dev.* **21**, 420 (2007).
14. Y. Boyarchuk, A. Salic, M. Dasso, A. Arnaoutov, *J. Cell Biol.* **176**, 919 (2007).
15. B. T. Roberts, K. A. Farr, M. A. Hoyt, *Mol. Cell. Biol.* **14**, 8282 (1994).
16. K. Jeganathan, L. Malureanu, D. J. Baker, S. C. Abraham, J. M. van Deursen, *J. Cell Biol.* **179**, 255 (2007).
17. H. Sharp-Baker, R. H. Chen, *J. Cell Biol.* **153**, 1239 (2001).
18. C. D. Warren *et al*., *Mol. Biol. Cell* **13**, 3029 (2002).
19. T. Kiyomitsu, C. Obuse, M. Yanagida, *Dev. Cell* **13**, 663 (2007).
20. S. Yamaguchi, A. Decottignies, P. Nurse, *EMBO J.* **22**, 1075 (2003).
21. C. Klebig, D. Korinth, P. Meraldi, *J. Cell Biol.* **185**, 841 (2009).
22. G. L. Williams, T. M. Roberts, O. V. Gjoerup, *Cell Cycle* **6**, 1699 (2007).
23. T. S. Kitajima, S. A. Kawashima, Y. Watanabe, *Nature* **427**, 510 (2004).
24. Z. Tang, Y. Sun, S. E. Harley, H. Zou, H. Yu, *Proc. Natl. Acad. Sci. U.S.A.* **101**, 18012 (2004).
25. T. S. Kitajima, S. Hauf, M. Ohsugi, T. Yamamoto, Y. Watanabe, *Curr. Biol.* **15**, 353 (2005).
26. J. Fernius, K. G. Hardwick, *PLoS Genet.* **3**, e213 (2007).
27. Z. Tang, H. Shu, D. Oncel, S. Chen, H. Yu, *Mol. Cell* **16**, 387 (2004).
28. Materials and methods are available as supporting material on *Science* Online.
29. P. Bernard, K. Hardwick, J. P. Javerzat, *J. Cell Biol.* **143**, 1775 (1998).
30. S. Hauf *et al*., *EMBO J.* **26**, 4475 (2007).
31. P. Bernard, J. F. Maure, J. P. Javerzat, *Nat. Cell Biol.* **3**, 522 (2001).
32. B. M. Kiburz *et al*., *Genes Dev.* **19**, 3017 (2005).
33. Y. Yamagishi, T. Sakuno, M. Shimura, Y. Watanabe, *Nature* **455**, 251 (2008).
34. H. P. Cam *et al*., *Nat. Genet.* **37**, 809 (2005).
35. J. N. Hirschhorn, A. L. Bortvin, S. L. Ricupero-Hovasse, F. Winston, *Mol. Cell. Biol.* **15**, 1999 (1995).
36. V. B. Indjeian, B. M. Stern, A. W. Murray, *Science* **307**, 130 (2005).
37. J. Lee *et al*., *Nat. Cell Biol.* **10**, 42 (2008).
38. E. Llano *et al*., *Genes Dev.* **22**, 2400 (2008).
39. H. Aihara *et al*., *Genes Dev.* **18**, 877 (2004).
40. A. L. Brittle, Y. Nanba, T. Ito, H. Ohkura, *Exp. Cell Res.* **313**, 2780 (2007).
41. A. C. Harvey, S. P. Jackson, J. A. Downs, *Genetics* **170**, 543 (2005).
42. We thank S. Hauf for critically reading the manuscript, F. Winston and the Yeast Genetic Resource Center for yeast strains, H. Masumoto for methods, and S. Ihara for injection instructions. We also thank all the members of our laboratory for their valuable support and discussion. This work was supported in part by the Japan Society for the Promotion of Science Research Fellowship (to. S.A.K. and Y.Y.) and Grant-in-Aid for Young Scientists (to K.I.), the Global Centers of Excellence Program, and a Grant-in-Aid for Specially Promoted Research (to Y.W.) from the Ministry of Education, Culture, Sports, Science and Technology of Japan.

Supporting Online Material

www.sciencemag.org/cgi/content/full/1180189/DC1
Materials and Methods
Figs. S1 to S18
Table S1
References

5 August 2009; accepted 6 November 2009
Published online 19 November 2009;
10.1126/science.1180189
Include this information when citing this paper.

Quantum Criticality in an Ising Chain: Experimental Evidence for Emergent E_8 Symmetry

R. Coldea,[1]* D. A. Tennant,[2] E. M. Wheeler,[1]† E. Wawrzynska,[3] D. Prabhakaran,[1] M. Telling,[4] K. Habicht,[2] P. Smeibidl,[2] K. Kiefer[2]

Quantum phase transitions take place between distinct phases of matter at zero temperature. Near the transition point, exotic quantum symmetries can emerge that govern the excitation spectrum of the system. A symmetry described by the E_8 Lie group with a spectrum of eight particles was long predicted to appear near the critical point of an Ising chain. We realize this system experimentally by using strong transverse magnetic fields to tune the quasi–one-dimensional Ising ferromagnet $CoNb_2O_6$ (cobalt niobate) through its critical point. Spin excitations are observed to change character from pairs of kinks in the ordered phase to spin-flips in the paramagnetic phase. Just below the critical field, the spin dynamics shows a fine structure with two sharp modes at low energies, in a ratio that approaches the golden mean predicted for the first two meson particles of the E_8 spectrum. Our results demonstrate the power of symmetry to describe complex quantum behaviors.

Symmetry is present in many physical systems and helps uncover some of their fundamental properties. Continuous symmetries lead to conservation laws; for example, the invariance of physical laws under spatial rotation ensures the conservation of angular momentum. More exotic continuous symmetries have been predicted to emerge in the proximity of certain quantum phase transitions (QPTs) (*1*, *2*). Recent experiments on quantum magnets (*3*–*5*) suggest that quantum critical resonances may expose the underlying symmetries most clearly. Remarkably, the simplest of systems, the Ising chain, promises a very complex symmetry, described mathematically by the E_8 Lie group (*2*, *6*–*9*). Lie groups describe continuous symmetries and are important in many areas of physics. They range in complexity from the U(1) group, which appears in the low-energy description of superfluidity, superconductivity, and Bose-Einstein condensation (*10*, *11*), to E_8, the highest-order symmetry group discovered in mathematics (*12*), which has not yet been experimentally realized in physics.

The one-dimensional (1D) Ising chain in transverse field (*10*, *11*, *13*) is perhaps the most-studied theoretical paradigm for a quantum phase transition. It is described by the Hamiltonian

$$H = \Sigma_i - JS_i^z S_{i+1}^z - hS_i^x \qquad (1)$$

where a ferromagnetic exchange $J > 0$ between nearest-neighbor spin-½ magnetic moments $\mathbf{S}_i$ arranged on a 1D chain competes with an applied external transverse magnetic field h. The Ising exchange J favors spontaneous magnetic order along the z axis ($|\uparrow\uparrow\uparrow \cdots \uparrow\rangle$ or $|\downarrow\downarrow\downarrow \cdots \downarrow\rangle$), whereas the transverse field h forces the spins to point along the perpendicular $+x$ direction ($|\rightarrow\rightarrow\rightarrow \cdots \rightarrow\rangle$). This competition leads to two distinct phases, magnetically ordered and quantum paramagnetic, separated by a continuous transition at the critical field $h_C = J/2$ (Fig. 1A). Qualitatively, the magnetic field stimulates quantum tunneling processes between ↑ and ↓ spin states and these zero-point quantum fluctuations "melt" the magnetic order at h_C (*10*).

To explore the physics of Ising quantum criticality in real materials, several key ingredients are required: very good one-dimensionality of the magnetism to avoid mean-field effects of higher dimensions, a strong easy-axis (Ising) character, and a sufficiently low exchange energy J of a few meV that can be matched by experimentally attainable magnetic fields (10 T ~ 1 meV) to access the quantum critical point. An excellent model system to test this physics is the insulating quasi-1D Ising ferromagnet $CoNb_2O_6$ (*14*–*16*), where magnetic Co^{2+} ions are arranged into near-isolated zigzag chains along the c axis with strong easy-

[1]Clarendon Laboratory, Department of Physics, University of Oxford, Oxford OX1 3PU, UK. [2]Helmholtz-Zentrum Berlin für Materialien und Energie, Lise Meitner Campus, Glienicker Str. 100, D-14109 Berlin, Germany. [3]H. H. Wills Physics Laboratory, University of Bristol, Bristol BS8 1TL, UK. [4]ISIS, Rutherford Appleton Laboratory, Chilton, Didcot OX11 0QX, UK.

*To whom correspondence should be addressed. E-mail: r.coldea@physics.ox.ac.uk
†Present address: Helmholtz-Zentrum Berlin für Materialien und Energie, Lise Meitner Campus, Glienicker Str. 100, D-14109 Berlin, Germany.

Phosphorylation of H2A by Bub1 Prevents Chromosomal Instability Through Localizing Shugoshin

Shigehiro A. Kawashima *et al.*

Science **327**, 172 (2010);
DOI: 10.1126/science.1180189